

ISOTHERMAL MODELS OF CHROMIUM (VI) ADSORPTION BY USING Fe₃O₄ NANOPARTICLES

Dang Tan Hiep¹, Bui Thi Hoa^{2,3}, Ngo Thi My Thanh⁴, Nguyen Anh Tien⁵,
Nguyen Viet Long⁶, Le Hong Phuc⁷, Bui Xuan Vuong^{8,9*}

¹Faculty of Chemical Engineering, Ho Chi Minh City University of Food Industry,
Ho Chi Minh City, 700000, Vietnam

²Institute of Theoretical and Applied Research, Duy Tan University, Hanoi,
100000, Vietnam

³Faculty of Natural Sciences, Duy Tan University, Da Nang, 550000, Vietnam

⁴Faculty of Chemical Technology and Food, Ho Chi Minh City Industry and Trade
College, 20 Tang Nhon Phu, District 9, Ho Chi Minh City, 700000, Vietnam

⁵Faculty of Chemistry, Ho Chi Minh City University of Education,
Ho Chi Minh City, 700000, Vietnam

⁶Department of Electronics and Telecommunication, Sai Gon University,
273 An Duong Vuong, District 5, Ho Chi Minh City, 700000, Vietnam

⁷Ho Chi Minh City Institute of Physics, Vietnam Academy of Science and Technology,
01 Mac Dinh Chi St, District 01, Ho Chi Minh City, 700000, Vietnam

⁸Department for Management of Science and Technology Development,
Ton Duc Thang University, Ho Chi Minh City, 700000, Vietnam

⁹Faculty of Applied Sciences, Ton Duc Thang University, Ho Chi Minh City, 700000,
Vietnam

Received 06.04.2020

Accepted 22.06.2020

Abstract

The ferromagnetic Fe₃O₄ nanoparticles with the average particle size of about 10 nm were used to adsorb chromium (VI) in aqueous solution. The equilibrium of Cr(VI) adsorption can be achieved at the pH value of 2.5, in the contact time of 120 minutes. The mechanisms of Cr(VI) adsorption were evaluated by 4 isothermal adsorption models Langmuir, Freundlich, Redlich-Peterson, and Temkin. The results showed that all four models are satisfied; especially, Redlich-Peterson is the most suitable model to describe the adsorption kinetic of Cr(VI) on ferromagnetic Fe₃O₄ nanoparticles.

Keywords: Fe₃O₄ ferromagnetic nanoparticles, adsorption, Cr(VI), equilibrium, Redlich-Peterson.

*Corresponding author: Bui Xuan Vuong, buixuanvuong@tdtu.edu.vn

Introduction

Industrial activities such as mining, processing and metallurgy, electroplating, tanning, texturing, and dyeing are the main causes leading to the accumulation of chromium in the environment [1-2]. In water, chromium normally exists in various forms such as Cr(III) (Cr^{3+} , $\text{Cr}(\text{OH})^{2+}$) and Cr(VI) (HCrO_4^- , CrO_4^{2-} , $\text{Cr}_2\text{O}_7^{2-}$), in which Cr(VI) is listed as one of the most 20 pollutants endangering human health [3]. Chromium (VI) can cause allergies, dermatitis, liver damage, and extremely dangerous diseases like cancer [3]. Currently, many chemical and physical methods have been used to remove Cr(VI) ions in water environments such as adsorption, ion exchange, dialysis, coagulation, precipitation, and separation [4-6]. Among them, the adsorption method is one of the most convenient, economical, and effective. In the literature, metal-organic frameworks (MOF) such as copper benzene 1,3,5-tricarboxylate (Cu-BTC) was used to remove Cr(VI) ions in aqueous solution with an adsorption capacity of 48.0 mg/g [7]. Composite of fly ash/chitosan experimentally adsorbed Cr(VI) with an adsorption capacity of 36.2 mg/g [8]. Melamine-formaldehyde resin with medium capillary structure was an interesting adsorbed material with very high adsorption capacity (66.7 mg/g) [9]. The nano-composite $\text{BaTiO}_3@\text{SBA-15}$ showed a high adsorption efficiency with 98% of Cr(VI) removal in 40 minutes [10]. The surface-modified MnFe_2O_4 nanoparticles were efficient absorbent for fast removal of Cr(VI) from wastewater, with an interesting adsorption capacity of 31.5 mg/g [11]. The development of nanotechnology has opened up a variety of effective adsorbents to remove toxic heavy metal ions. Nano-materials can be easily synthesized at a low cost. Moreover, due to their small sizes and thus large specific surface areas, nanomaterials have strong adsorption capacities and reactivity [12-13]. Typically, ferromagnetic Fe_3O_4 nanoparticle exhibits unique physical and chemical properties such as electronic structure change, large specific surface area and good adsorption capacity [6, 14]. Thank magnetic properties, it can be easily separated and refined during the experiment. Depending on the synthesis process, ferromagnetic Fe_3O_4 and modified Fe_3O_4 nanoparticles show different morphologies of size and structure, resulting in different adsorption capacity [13-17].

In this study, ferromagnetic Fe_3O_4 nanoparticles with an average particle size of 10 nm were used to adsorb Cr(VI) in aqueous solution. The factors affecting the Cr(VI) adsorption such as pH, contact time, and initial concentration of Cr(VI) solutions were investigated. The mechanisms of Cr(VI) adsorption onto ferromagnetic Fe_3O_4 nanoparticles were studied and evaluated by four isothermal adsorption models Langmuir, Freundlich, Redlich-Peterson, and Temkin.

Materials and methods

Materials

Iron (III) chloride hexahydrate ($\text{FeCl}_3 \cdot 6\text{H}_2\text{O}$, $\geq 98\%$, Sigma-Aldrich); iron (II) chloride tetrahydrate ($\text{FeCl}_2 \cdot 6\text{H}_2\text{O}$, $\geq 99\%$, Merck); ammonia solution (NH_4OH , 25 - 28%, 0.91 g/mL, Merck); potassium chromate (K_2CrO_4 , $\geq 98\%$, Merck); 1,5-diphenylcarbazide ($\text{C}_6\text{H}_5\text{NHNHCONHNHC}_6\text{H}_5$, $\geq 99\%$, Sigma-Aldrich); phosphoric acid (H_3PO_4 , 85%, Merck); sodium hydroxide (NaOH , $\geq 99\%$, Merck); nitric acid (HNO_3 , 70 %, Merck).

Synthesis of ferromagnetic Fe₃O₄ nanoparticles

The Fe₃O₄ material was synthesized by dissolving a mixture of FeCl₃ and FeCl₂ in boiling water. The reaction system was stirred until the mixture was completely dissolved. Then, the NH₄OH solution was quickly added to the reaction mixture and continued to stir for 10 minutes. After that, the precipitation was collected quickly by placing a magnet outside the beaker. The precipitation was washed with distilled water to remove residual ions from the mixture and then dried in a vacuum desiccator. Finally, the obtained crystals of Fe₃O₄ were ground to a fine powder.

Experiments of Cr(VI) adsorption

The Cr(VI) solutions were made by dissolving potassium chromate salt K₂CrO₄ in distilled water with concentrations of 20, 40, 60, 80, 100, 120, 140, 160, 180 and 200 mg/L. The adsorption experiment was effectuated by immersing 0.1 g ferromagnetic Fe₃O₄ nanoparticles in 40 ml of Cr(VI) solution. The mixture was stirred at 100 rpm, at room temperature of 32.2 °C. The quantity of Cr(VI) in the solution before and after adsorption by ferromagnetic Fe₃O₄ nanoparticles was determined by measuring the absorbance of the red-violet complex formed by the reaction of Cr(VI) with 1, 5-diphenylcarbazide in phosphoric acid at 544 nm on an atomic absorption spectrometer (AA-7000-Shimadzu). The adsorption efficiency H (%) and the adsorption capacity q (mg/g) are calculated by two following formulas:

$$H\% = \frac{(C_0 - C)}{C_0} \cdot 100 \quad 1$$

$$q = \frac{(C_0 - C) V}{m} \quad 2$$

where C₀ and C (mg/L) are the concentrations of Cr(VI) solution before and after adsorption, V(L) is the volume of Cr(VI) solution, m (g) is the mass of the ferromagnetic Fe₃O₄ adsorbent.

Evaluation methods

The crystalline structure of powdered nanoparticles was characterized by the XRD method, performed on XRD-D8 ADVANCE (Brucker, Germany). The size of the Fe₃O₄ nanoparticles was determined by the TEM method, using the JEM-1400-JEOL (Japan) equipment system. The specific surface area was checked by the BET method, using Nova station A equipment, version 9.0 (Quantachrome Firm). The quantity of Cr(VI) in the solution before and after adsorption by Fe₃O₄ nanoparticles was found out by measuring the absorbance of the red-violet complex formed by the reaction of chromium (VI) with 1,5-diphenylcarbazide in phosphoric acid at 544 nm on an atomic absorption spectrometer (AA-7000-Shimadzu).

Results and discussion

Characterization of ferromagnetic Fe₃O₄ nanoparticles

The crystallinity of synthesized Fe₃O₄ nanoparticles can be identified via XRD analysis. The XRD patterns of synthesized Fe₃O₄ nanoparticles are shown in Figure 1. The diffraction peaks of synthesized Fe₃O₄ were detected at 2θ = 30°, 36°, 43°, 57°, and 63°, which are assigned to the crystal planes of (220), (311), (400), (511), and (440),

respectively (JCPDS file no. 75-0033). The strong and sharp peaks obtained from the XRD diagram confirmed the high crystallinity of ferromagnetic Fe₃O₄ nanoparticles. The size and morphology of the synthesized Fe₃O₄ nanoparticles were analyzed by using the TEM technique. The observation showed that Fe₃O₄ nanoparticles were in spherical shapes with an average size of about 10.0 nm (Figure 2).

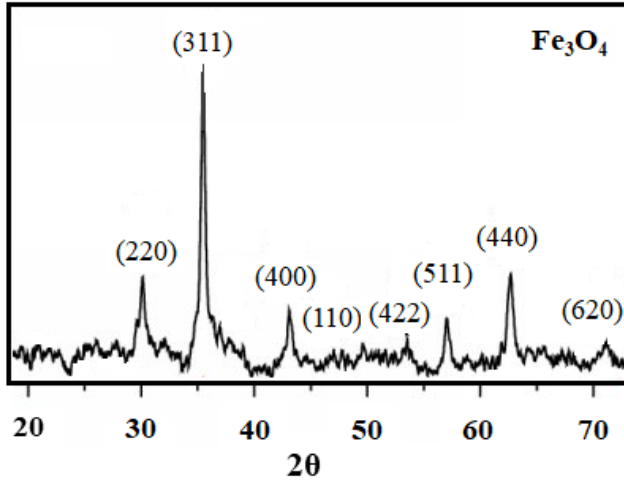


Fig. 1. XRD diagram of ferromagnetic Fe₃O₄ nanoparticles.

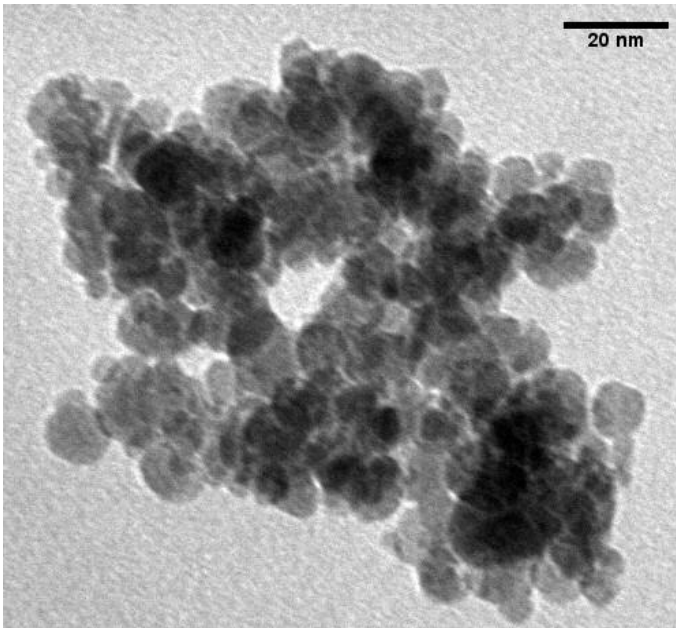


Fig. 2. TEM micrograph of ferromagnetic Fe₃O₄ nanoparticles.

Effect of pH on Cr(VI) adsorption by Fe_3O_4 nanoparticles

In aqueous solution, the adsorption efficiency of ions such as metal cations and inorganic anions in free or complex forms was influenced by various factors such as the quantity of ion in solution, pH, and other co-existing ions [18-19]. In particular, pH plays an important role relating to the adsorption mechanism. Based on pH value, physical and chemical interactions of substances in solution with active adsorbent centers can be interpreted. Figure 3 shows Cr(VI) adsorption efficiency at different pH from 2.0 to 10.0. The best adsorption efficiency was achieved at a pH of 2.5 (43.2%). Then, the adsorption efficiency decreased as increasing the pH value and rapidly decreased in the range of pH from 7 to 10. The surface charge of the adsorbent can explain the dependence of Cr(VI) adsorption efficiency on pH. In general, the surface of metal oxides is covered with hydroxyl groups, which change at different pH ranges. At the isoelectric point pH_{pzc} , the surface charge will be neutral. According to the literature [20], ferromagnetic Fe_3O_4 has an isoelectric point around 6.5. At pH lower than pH_{pzc} , the adsorbent surface is a positive charge, and anionic adsorption will occur due to electrostatic attraction. In contrast, at pH higher than pH_{pzc} , the adsorbent surface is a negative charge, cationic adsorption appears. In the case of chromium (VI) adsorption, the adsorption efficiency decreases with increasing pH, probably due to high concentrations of OH^- ions, which will compete for adsorption centers with Cr(VI) in CrO_4^{2-} solution. In other words, when the iron oxide surface is negatively charged ($pH > pH_{pzc}$), the electrostatic repulsion between adsorbed $HCrO_4^-$ and CrO_4^{2-} ions with the adsorbent surface increases, the adsorption efficiency decreases.

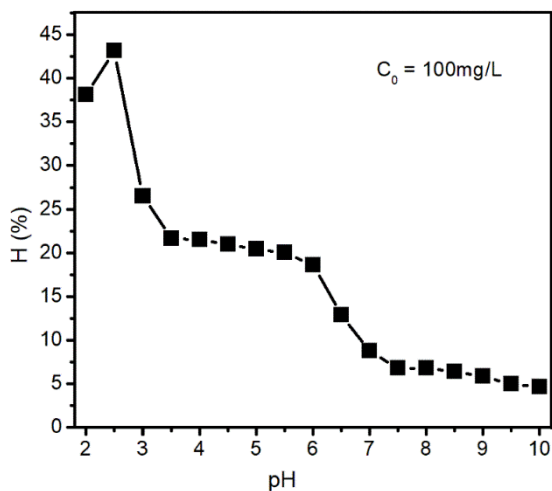


Fig. 3. Effect of pH on Cr(VI) adsorption efficiency H (%), C_0 refers to the concentration of Cr(VI) solution before adsorption.

Effect of time on Cr(VI) adsorption efficiency

At an optimal value of pH, Cr(VI) adsorption efficiency by ferromagnetic Fe_3O_4 nanoparticles at different times was investigated (Figure 4). The results presented that at the beginning, the adsorption rate significantly increased, and reached equilibrium status at $t = 120$ minutes. Therefore, 120 minutes is chosen as the time of adsorption equilibrium.

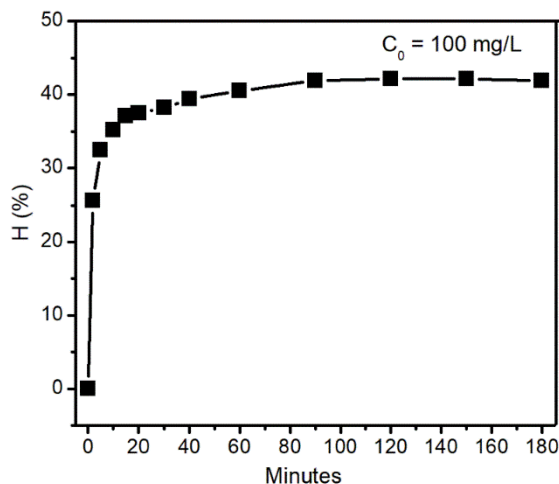


Fig. 4. Effect of time on Cr(VI) adsorption efficiency ($H\%$), C_0 refers to the concentration of the Cr(VI) solution before adsorption.

Equilibrium of Cr(VI) adsorption – Isothermal studies

Table 1. Adsorption parameters for isothermal models.

| C_0 (mg/L) | C_e (mg/L) | $\text{Ln}C_e$ | q_e (mg/g) | $\text{Ln}q_e$ | C_e/q_e (g/L) |
|-----------------|-----------------|----------------|-----------------|----------------|--------------------|
| 20 | 4.03 | 1.39 | 6.37 | 1.85 | 0.63 |
| 40 | 9.64 | 2.27 | 12.15 | 2.50 | 0.79 |
| 60 | 25.53 | 3.24 | 13.79 | 2.62 | 1.85 |
| 80 | 41.89 | 3.74 | 15.18 | 2.72 | 2.76 |
| 100 | 59.41 | 4.08 | 16.23 | 3.10 | 3.66 |
| 120 | 76.71 | 4.34 | 17.28 | 2.85 | 4.44 |
| 140 | 92.37 | 4.53 | 19.03 | 2.95 | 4.85 |
| 160 | 109.19 | 4.69 | 20.24 | 3.00 | 5.40 |
| 180 | 126.25 | 4.84 | 21.41 | 3.06 | 5.90 |
| 200 | 142.38 | 4.96 | 23.00 | 3.14 | 6.19 |

C_0 (mg/L): initial concentration of Cr(VI) solution, C_e (mg/L): equilibrium concentration of Cr(VI) solution, q_e (mg/g): maximum adsorption capacity at equilibrium time.

The process of chromium adsorption on 0.1g of ferromagnetic Fe_3O_4 was carried out at optimal pH = 2.5, room temperature = 32.2 °C and $t = 120$ minutes. The concentration of chromium solution was tested from 20 to 200 mg/L. The volume of the chromium solution is 40 mL. Adsorption parameters corresponding to the initial concentration of chromium solution was presented in Table 1.

Langmuir isothermal adsorption model

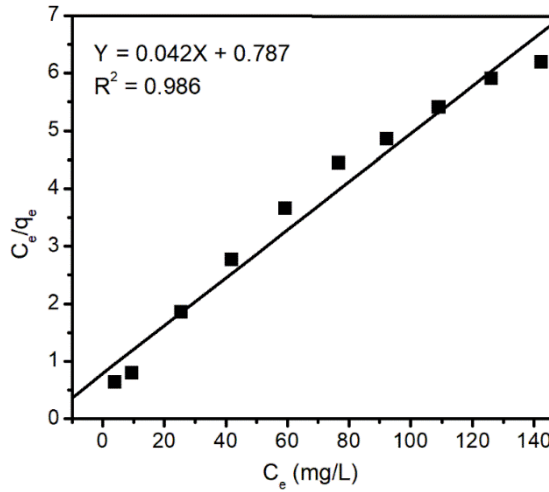


Fig. 5. Langmuir isothermal adsorption model, C_e (mg/L): equilibrium concentration of Cr(VI) solution, q_e (mg/g): maximum adsorption capacity at equilibrium time.

According to the Langmuir isothermal adsorption model, the adsorption of metal ions is assumed to occur on a homogeneous surface, monolayer surface of the adsorbent without any interaction between adsorbed ions [21]. A linear equation shows the Langmuir isothermal adsorption model:

$$\frac{C_e}{q_e} = \frac{C_e}{q_m} + \frac{1}{K_L \cdot q_m} \tag{3}$$

where K_L is the Langmuir adsorption constant, q_m is the maximum adsorption capacity.

The Langmuir isothermal adsorption model was shown in figure 5. The high value of the correlation coefficient (R² = 0.986) indicated that the Langmuir isothermal model is suitable for Cr(VI) adsorption by ferromagnetic Fe₃O₄ nanoparticles. The maximum adsorption capacity q_m was 24.03 mg/g, the Langmuir adsorption constant is 0.053.

Freundlich isothermal adsorption model

According to the Freundlich isothermal adsorption model, the adsorption is assumed that adsorption occurs on the inhomogeneous surface of the material [21-22].

The following equation represents the linear equation:

$$\text{Ln}q_e = \text{Ln}K_F + \frac{1}{n} \cdot \text{Ln}C_e \tag{4}$$

where n is the exponential constant in the Freundlich equation, which characterizes for heterogeneous energy of the adsorbed surface. K_F is the Freundlich constant to show the relative adsorption capacity of adsorbent materials. The Freundlich model was chosen to evaluate the adsorption intensity of the adsorbate on the surface of the adsorbent. The graph of the Freundlich isothermal equation was shown in Figure 6.

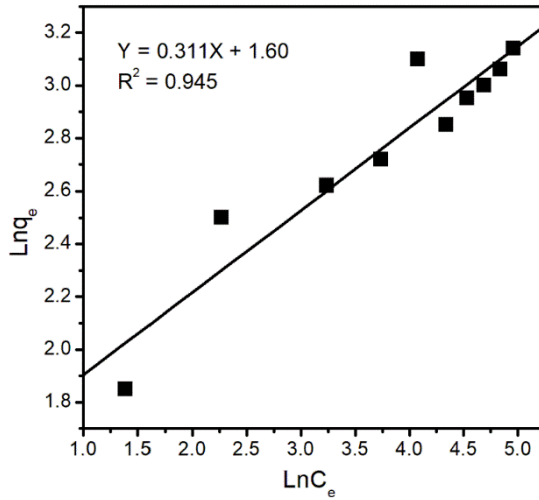


Fig. 6. Freundlich isothermal adsorption model, C_e (mg/L): equilibrium concentration of Cr(VI) solution, q_e (mg/g): maximum adsorption capacity at equilibrium time.

The value correlation coefficient R^2 in the Freundlich model is lower than that in the Langmuir adsorption isothermal model. The value of $1/n$ in the case of adsorption on liquid/solid boundary is in the range of 0.1 - 0.5 [22]. In this study, the calculated value of $1/n$ was 0.311, showing a good fit for the above range, indicating that the Freundlich adsorption isothermal model can be used to describe the chromium (VI) adsorption process by ferromagnetic Fe_3O_4 nanoparticles.

Redlich-Peterson isothermal adsorption model

Redlich-Peterson isothermal adsorption model is an isothermal model combining Langmuir and Freundlich models [23]. The Redlich-Peterson equation is described as follows:

$$\text{Ln} \left(K_{RP} \frac{C_e}{q_e} - 1 \right) = \beta \text{Ln}C_e + \text{Ln}\alpha_{RP} \tag{5}$$

where K_{RP} (L/g), α_{RP} (L/mg), and β are constants. β is in the range between 0 and 1. The Redlich-Peterson isothermal adsorption model accesses the Freundlich model at

high concentration (β approaches to 0) and accesses the Langmuir model at low concentration (β approaches to 1).

Chromium adsorption, according to the Redlich-Peterson isothermal adsorption model is shown in Figure 7. Linear correlation with high correlation coefficient $R^2 = 0.994$ indicating that the Redlich-Peterson isothermal adsorption model is also suitable to describe the chromium adsorption on ferromagnetic Fe₃O₄ nanoparticles.

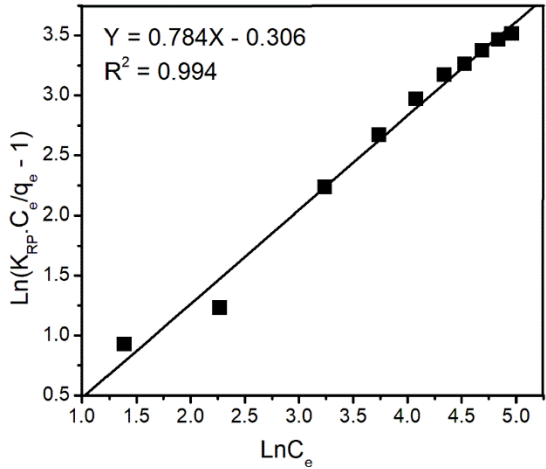


Fig. 7. Redlich-Peterson isothermal adsorption model, K_{RP} is constant, C_e (mg/L): equilibrium concentration of Cr(VI) solution, q_e (mg/g): maximum adsorption capacity at equilibrium time.

Temkin isothermal adsorption model

Temkin isothermal adsorption was used to apply for chemical adsorption [23]. This model shows that the heat energy of all molecules absorbed on the surface decreases linearly with the coverage area due to the interaction between adsorbent and adsorbate. The Temkin equation is described as follows:

$$q_e = B \ln K_T + B \ln C_e \tag{6}$$

where $B = RT / b_T$, T is the adsorption temperature (Kelvin), R is the gas constant (8.314.10⁻³ kJ / mol·K), b_T is the Temkin constant kJ/mol).

Figure 8 indicated $K_T = 1.31$ (L/mg), $b_T = 0.63$ (mol/kJ) and $R^2 = 0.970$. Empirical data analysis indicated that all four isothermal adsorption models are suitable to describe chromium (VI) adsorption by ferromagnetic Fe_3O_4 nanoparticles, in which the Redlich-Peterson model is the best fit.

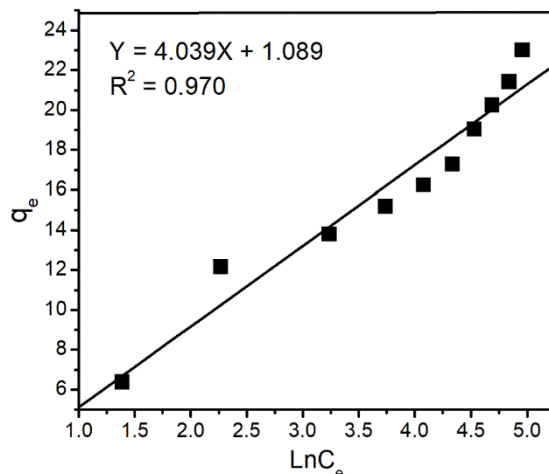


Fig. 8. Temkin isothermal adsorption model, C_e (mg/L): equilibrium concentration of Cr(VI) solution, q_e (mg/g): maximum adsorption capacity at equilibrium time.

Conclusion

This study investigated chromium (VI) adsorption on ferromagnetic Fe_3O_4 nanoparticles in aqueous solution. The factors affecting Cr(VI) adsorption such as pH, exposure time, and initial concentration of Cr(VI) solutions, were evaluated. Experimental data were analyzed by 4 isothermal adsorption models Langmuir, Freundlich, Redlich-Peterson, and Tempkin. The results show that in the optimal conditions (pH = 2.5, stirring speed = 100 rpm, stirring time = 120 minutes, adsorbent mass $Fe_3O_4 = 0.1$ grams), the Cr(VI) adsorption process can be well fitted by all 4 isothermal models. Interestingly, the Redlich-Peterson model shows the best suitability for chromium (VI) adsorption with a very high correlation coefficient ($R^2 = 0.994$).

References

- [1] Y. Wang, J. Shi, H. Wang, Q. Lin, X. Chen, Y. Chen: *Ecotox Environ Safe*, 67 (2007) 75–81.
- [2] A. R. Wadhawan, A. T. Stone, E. J. Bouwer: *Environ Sci Technol*, 47 (2013) 8220–8228.
- [3] B. Dhal, H. N. Thatoi, N. N. Das, B. D. Pandey: *J Hazard Mater*, 250 (2013) 272–291.
- [4] L. F. Feng, W. Qi: *J Environ Manag*, 92 (2013) 407–18.
- [5] L. Zhou, C. Gao, W. J. Xu: *App Mater Inter*, 2 (2010) 1483–1491.
- [6] H. Gao et al: *RSC Adv*, 5 (2015) 60033–60040.
- [7] A. Maleki, B. Hayati, M. Naghizadeh, S. W. Joo: *J Ind Eng Chem*, 28 (2015) 211–216.
- [8] A. Adamczuk, D. Kolodynska: *Chem Eng J*, 274 (2015) 200–212.
- [9] L. V. Zhongfei et al: *RSC Adv*, 5 (2015) 18213–18217.
- [10] V. Kumari, M. Sasidharan, A. Bhaumik: *Dal Trans*, 44 (2015) 1924–1932.
- [11] J. Hu, I. M. C. Lo, G. Chen: *Langm*, 21 (2005) 11173–11179.
- [12] S. R. Kanel, J. M. Greneche, H. Choi: *Environ Sci Tech*, 40 (2006) 2045–2050.
- [13] P. Wang, M. C. Irene: *Water Res*, 43 (2006) 727–734.
- [14] Y. H. Chen, D. Y. Liu, J. F. Lee: *Phys Chem Miner*, 45 (2018) 907–913.
- [15] Y.F. Shena, J. Tang, Z. H. Niea, Y. D. Wanga, Y. Renc, L. Zuo: *Sep Purif Technol*, 68 (2009) 312–319.
- [16] B. S. Damascenoa, A. F. V. Silvab, A. C. V. Araujo: *J Environ Chem Eng*, 8 (2020) 103994.
- [17] X. Liua, J. Tianaa, Y. Lia, N. Suna, S. Mia, Y. Xiea, Z. Chen: *J Hazard Mater*, 373 (2019) 397–407.
- [18] T. Shahriari, G. N. Bidhendi, N. Mehrdadi, A. Torabian: *Inter J Environ Sci Tech*, 11 (2014) 349–356.
- [19] E. Demibas, M. Kobya, E. Sentuk, T. Ozkan: *Water SA*, 30 (2004) 533–539.
- [20] V. Miroslava et al, *Water treatment technologies for the removal of high-toxicity pollutants*, The NATO Science for Peace and Security Series C: Environmental Security book series NAPSC, 2008, 13–17.
- [21] K. Y. Foo, B. H. Hameed: *Chem Eng J*, 156 (2010) 2–10.
- [22] S. S. Baral, N. S. Das, R. Pradip: *Biochem Eng J*, 31 (2006) 216–222.
- [23] N. Ayawei et al: *J Chem*, 1 (2017) 1–11.



Creative Commons License

This work is licensed under a Creative Commons Attribution 4.0 International License.